Iranian Journal of Science
https://doi.org/10.1007/s40995-023-01543-2

RESEARCH PAPER

A Novel Oil Sorbent Based on Butyl Acrylate Grafting onto Cellulose of Disposable Diaper

Nguyen Trung Duc[1] · Nguyen Thanh Tung[1] · Pham Thi Thu Ha[1] · Le Duc Giang[2] · Dau Xuan Duc[2] · Ninh The Son[1]

Received: 2 January 2023 / Accepted: 15 October 2023

Abstract
For the first time, a potential co-polymer for oil spill cleanup has been successfully synthesized by the graft co-polymerization of butyl acrylate (BA) onto cellulose from disposable diaper (DD) using 2,2'-azobisisobutyronitrile (AIBN) as initiator in the presence of cross-linkers divinyl benzene (DVB) or methylene bisacrylamide (MBA). The copolymeric synthesis has been controlled by the concentration of monomer BA and AIBN, reaction time, temperature. The highest graft yield (GY) of 41.50% is obtained with the optimal condition: C_{AIBN} = 0.04 mol/L, C_{BA} = 1.50 mol/L, 180 min at 75 °C. The structure of co-polymer DD-*g*-poly(BA) is characterized by the FT-IR (Fourier transform infrared spectroscopy), SEM (scanning electron microscopy), XRD (X-ray diffraction), TGA (thermogravimetric analysis), and BET surface area analysis. In the presence of the better cross-linker DVB (1.5%) and contact time of about 25 min, the maximal OSC (oil sorption capacity) of co-polymer toward crude and vegetable oils is 23.56 and 25.63 g/g, respectively. The OSC is reduced when sorbent dosage increased, but it increases with increasing the temperature and reaches maximum at 40 °C. The reusability of this co-polymer is characteristic of seven sorption/desorption cycles. Importantly, the Langmuir monolayer, chemisorption, and pseudo-second-order model are likely the best approaches to describe absorption kinetics of DD-*g*-poly(BA).

Keywords Oil sorbent · Graft co-polymerization · Cellulose · Disposable diaper

1 Introduction

Crude oil is one of the most essential energy sources. For a long time, it has been utilized as main materials for transportation vehicles, and the production of various products. In the modern industrial world, there has been an increase in the demand for oil. The oil spills, on the other hand, will occur during the production, transportation, and storage, on the one hand, have directly affected to aquatic life, local economy, tourism, and recreational activities. Oil sorbents can be divided into synthetic and natural categories. Synthetic materials are the most prevalent products used for oil sorbents. However, they are non-biodegradable and quite expensive. Therefore, the search for oil sorbents from natural resources has drawn much interest to scientists.

DD was used once, and then discarded without being recycled (Sotelo-Navarro et al. 2017; Frency et al. 2013). DD trashes account for 3.5 million tons (2–7%) of total municipal solid waste, which is reasonable for environmental pollution (Umberto et al. 2016; Ching Khoo et al. 2019). As far as we know, the combustion of DDs and other solid trashes have possibly generated various hazardous gases, such as NO_2, SO_2, HCl, dioxins, CO_2, and ash (Joan et al. 2013; Khandelwal et al. 2019; Mendoza et al. 2019a, 2019b). DDs can endure up to 500 years because of the inclusion of synthetic polymers (Mohamad et al. 2017).

✉ Nguyen Thanh Tung
nttung@ich.vast.vn

✉ Ninh The Son
ntson@ich.vast.vn

[1] Institute of Chemistry, Vietnam Academy of Science and Technology (VAST), 18 Hoang Quoc Viet, Caugiay, Hanoi, Vietnam

[2] Faculty of Chemistry, College of Education, Vinh University, 182 Le Duan, Vinh, Nghean, Vietnam

Published online: 06 November 2023

Graft copolymerization is a synthetic process that demonstrates the covalent bonding of side chains to the polymeric backbone. By this, it would improve the beneficial physical and/or chemical properties of copolymers. Most of cellulosic graft copolymerization reactions are ruled by radical reactive mechanism, in which vinyl derivatives and AIBN have been used as the respective monomers and initiators (David and Samuel 2001). Hydrophobic monomer BA, among vinyl monomers, is appropriate for naturally synthesized copolymers because it promotes swelling behavior and product sorption efficiency (Vijay et al. 2013a). It should be noted that the addition of the cross-linkers to grafting procedures, such as DVB and MBA derivatives, has a direct impact on the oil sorption of co-polymers (Hua et al. 2013).

Many attempts are now being performed to utilize DD trashes. Energy pellets, anode material for lithium-ion batteries, concrete admixture, catalysts, soil amendment, and mushroom cultured substrates were among non-diaper goods created from DDs (Jee et al. 2021). The current research is established to synthesize a novel oil sorbent by grafting copolymerization of monomeric BA onto the cellulosic backbone of the DP material, using initiator AIBN, as well as the presence of cross-linkers DVB or MBA (Fig. 1). The FT-IR, SEM, XRD, TGA, and BET surface area analysis have been used to characterize the graft co-polymer DD-*g*-poly(BA). Absorption capacity on both vegetable and crude oils, as well as reusability of the synthesized product were studied and evaluated.

2 Materials and Methods

2.1 Devices and Chemicals

The Nicolet iS50 FT-IR spectrometer (4000–400 cm^{-1}) was used to record the IR spectra. The samples were mixed with dried KBr powder. The SNE-3200M scanning electron microscope was used to view morphological illustration, while the ARL EQUINOX 100 X-ray diffractometer was applied to the X-ray diffraction study with scanning range from 5° to 50°. Thermogravimetric data were obtained by the SDTGA 6000A thermal analyzer. BET surface area was measured from nitrogen adsorption/desorption at 77 K using the Micromeritics® TriStar II Plus. All samples were analyzed in air, heating rate 10°/min from room temperature to 800 °C.

All chemicals, consisting of BA, DVB, MBA, CH_3COOH, CH_3COCH_3, HNO_3, EtOH, and *N*,*N*-dimethyl formamide (DMF), were supplied by Sigma-Aldrich.

2.2 Cellulosic Extraction

The method is carried out following previous report with few modifications (Trilokesh et al. 2021). Briefly, the disposable diaper was washed several times by water, and dried overnight at 60°C. The swelling SAP (Super Absorbent Polymer) was physically removed. The remaining diaper was then decreased in the size of 0.5 × 0.5 cm. This milled diaper (3.0 g) was added to 60 mL of CH_3COOH

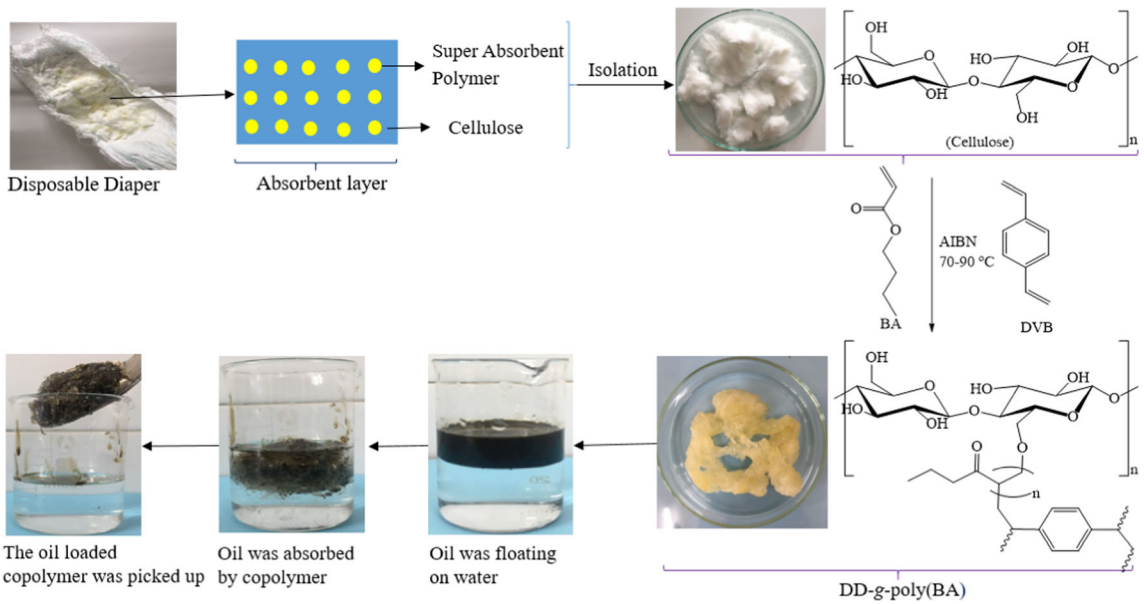

Fig. 1 Synthetic procedure of co-polymer DD-*g*-poly(BA) from raw material DD and its crude oil absorption illustration

(82%) and HNO_3 (72%) mixture (1:20 w/v), with the rate of HNO_3 to CH_3COOH being 1:10 (v/v). For 20 min, the acid suspension was maintained in a hot air oven at 120 °C. The suspension was then filtered using vacuum with a 0.20 μm pore size filter membrane, and the cellulose filter cake was collected. To eliminate the excess acids, the obtained cellulose was repeatedly rinsed with distilled water, and then with EtOH. The washing process was repeated until the cellulose was completely white.

2.3 Synthesis

The synthetic procedure was carried out following previous reports with a few modifications (Nguyen et al. 2021a; Qinhui et al. 2013; Saisai et al. 2019). The reaction was performed in nitrogenous medium in 200-mL bottom flask aided by a condenser. 0.6 g of DD (a_1) was soaked and stirred in DMF (15 mL) for 4.5 h. The pre-calculated amounts of monomeric BA, and cross-linked agent DVB or MBA were then added. The reaction temperature was regulated from 70 to 90 °C. The pre-calculated amount of AIBN was continued to add. The graft product BD-*g*-poly(BA) was mixed with EtOH (220 mL) for precipitation after the required reaction duration. To remove the homopolymer, it was then washed with EtOH (150 mL). Lastly, the co-polymer was dried to a constant weight a_2 under vacuum at 55 °C (Fig. 1). In the same model, the product after being precipitated in EtOH was extracted with CH_3COCH_3 (100 mL) using a Soxhlet apparatus in 18 h to discard the homo-polymer. The copolymer was then chopped into small pieces, and dried under vacuum at 55 °C to a constant weight (a_3).

The graft yield (GY) was denoted as Eq. 1:

$$\mathrm{GY}\ (\%) = (a_2 - a_1)/a_1 \times 100 \tag{1}$$

The gel fraction (GF) was ruled by the following Eq. 2:

$$\mathrm{GF}\ (\%) = \frac{a_3}{a_2} \times 100 \tag{2}$$

2.4 Preparation of Test Oils

Crude oil was supplied by Vietnam Petroleum Institute, whereas vegetable oil was derived from Tuong An Vegetable Oil Joint Stock Company. Densities of the oils were measured using a gravimetric method. The surface tension and density of the liquids were measured using Laryee JYW-200A Tensiometer. The viscosity of the oil was measured using Brookfield viscometer. The properties of crude and vegetable oils used in this study are given in Table 1. These two oils were used without modification.

2.5 Batch Oil Sorption and Reusability Measurements

Two different types of oil, including vegetable and crude oils, were employed to evaluate the oil sorption behavior of sorbent (co-polymer) (Yue et al. 2014; Nguyen et al. 2022a, b, ASTM D1533-00 2005). In a 150-mL conical flask, a known weight of vegetable oil or crude oil was combined with 150 mL of synthetic seawater (35 g of NaCl in 1000 mL distilled water) for 10 min at 150 rpm over a magnetic stirrer. The agitation can cause the oil to rise to the water's surface, forming an oil coating. Co-polymer (0.1–0.5 g) was placed in the oil/water mixture for 0–35 min at 25–55 °C while being agitated. The sample was then taken out of the flask using a mesh screen, drained for 1 min, and weighed.

The oil sorption capacity (OSC) is calculated by weighing the samples before and after the absorption, and followed by Eq. 3:

$$\mathrm{OSC} = (R_T - R_W - R_A)/R_A \tag{3}$$

where R_T stands for the total weight (g) of the oil + water + dry sorbent, R_A represents the weight of dry sorbent (g), and R_W denotes the weight of absorbed water (g). The amount of absorbed water is calculated via the extraction isolation using solvent *n*-hexane.

Regarding reusability: Oil-loaded co-polymer was put into a sand core funnel, and filtrated for 10 min using a vacuum pump (Wang et al. 2013). The resultant co-polymer was weighted to collect the mass of remnant oil. The action was repeated. However, a certain amount of oil could be adsorbed on the surface of co-polymer. The oil sorption capacity and oil recovery efficiency after seven sorption/desorption cycles was evaluated (Wang et al. 2013; Nguyen et al. 2021a, 2021b; Viju et al. 2019).

3 Results and Discussion

3.1 Effect of Reaction Time

The GY grows with reaction time in general, peaking at 180 min (Fig. 2). Beyond 180 min, the GY rate remains

Table 1 Physical properties of used oils

No	Density (g/cm^3)	Viscosity (MPa s)	Surface tension (cN cm^{-1})
Vegetable oil	0.85	38.56	2.4×10^{-2}
Crude oil	0.93	175.2	3.2×10^{-2}

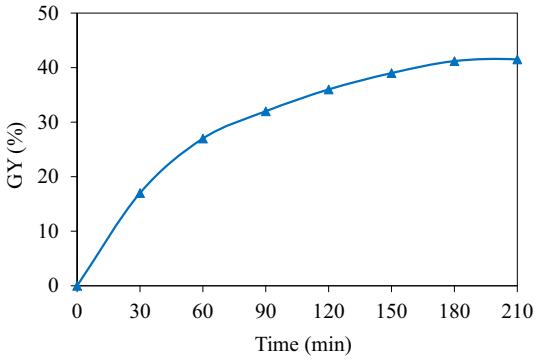

Fig. 2 Effect of reaction time on the GY. C_{BA} = 1.50 mol/L, C_{AIBN} = 0.04 mol/L, and reaction temperature = 75 °C

constant. The high concentration of BA and the great number of grafting sites in cellulosic backbone can be seen as a main cause for an increase in the GY percent in the early stage of reaction (Nguyen et al. 2022a). However, homo-polymeric reactions among monomeric BAs might be greater over co-polymeric reactions when the reaction time is longed (Nguyen et al. 2022b). As a result, a reaction time of 180 min might be considered the ideal setting for maximizing the GY (Fig. 3).

3.2 Effect of Temperature

The GY increases as the reaction temperature rises from 65 to 90 °C, peaking at 41.50% at 75 °C. Beyond 75 °C, however, the GY is observed to be reduced. As the reaction temperature rose in the first stage (65–75 °C), the diffusion of monomer and initiator to the cellulosic backbone and their interactions with cellulosic macro-radicals are accelerated (Khullar et al. 2008). However, as the reaction temperature is increased (75–90 °C), the GY decreases, which is most likely owing to the production of an unstable complex by the initiator, and the dominance of the termination processes (Khullar et al. 2008).

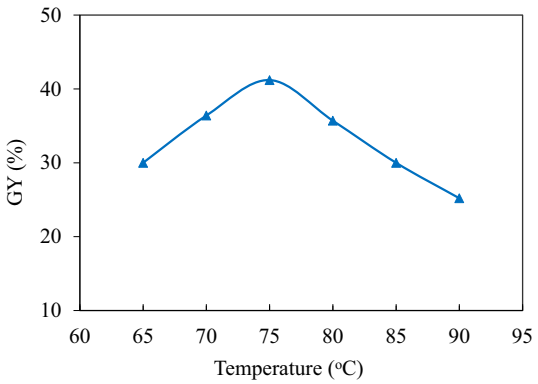

Fig. 3 Effect of temperature on the GY. C_{AIBN} = 0.04 mol/L, C_{BA} = 1.50 mol/L, and reaction time = 180 min

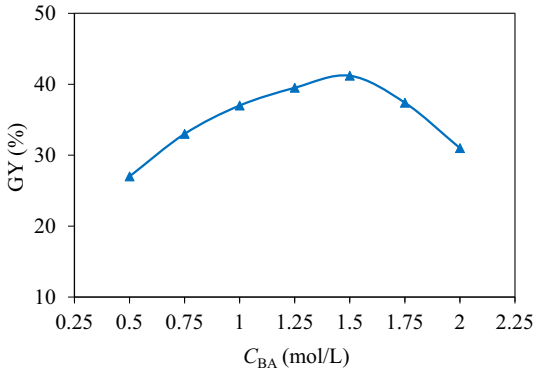

Fig. 4 Effect of monomer concentration on the GY. C_{AIBN} = 0.04 mol/L, reaction time = 180 min, and reaction temperature = 75 °C

3.3 Effect of Monomer Concentration

Figure 4 shows the effect of C_{BA} on the GY. The GY grows up from the lowest value of 27.0% at C_{BA} = 0.50 mol/L, and reaches the highest value of 41.50% at C_{BA} = 1.5 mol/L. However, further increase in C_{BA} from 1.5 to 2.0 mol/L results in a decrease in the GY. This trend can be explained by the fact that a great amount of radicals reaches cellulosic backbone at first stage, causing the grafting to grow (Khullar et al. 2008). However, as the monomer concentration rises, homo-polymerization takes precedence over graft co-polymerization, resulting in the lower GY. The availability of C_{BA} around cellulosic macro-radicals, which is a prerequisite for graft initiation and propagation, thereby increasing the GY. Because cellulosic macro-radicals are generally static, BA molecule must be in close proximity for grafting to occur. As a result, the creation of lengthy chains can be blamed for the increase in the GY (Khullar et al. 2008).

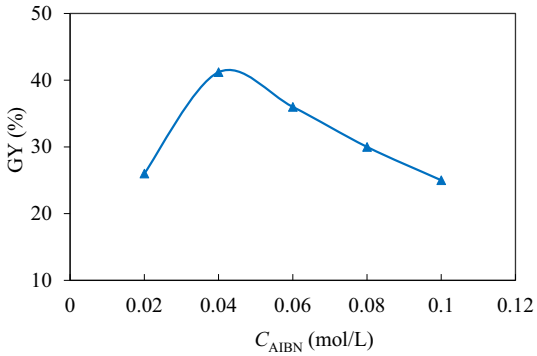

Fig. 5 Effect of initiator concentration on the GY. C_{BA} = 1.50 mol/L, reaction time = 180 min, and reaction temperature = 75 °C

3.4 Effect of Initiator Concentration

The effect of C_{AIBN} on the GY has shown in Fig. 5 when C_{AIBN} changed from 0.02 to 0.1 mol/L. When C_{AIBN} increased from 0.02 to 0.04 mol/L, the GY correspondingly increased and accounted for the maximal 41.50%, similar to the other experimental parameters. The GY steadily decreases when C_{AIBN} rises over 0.04 mol/L. AIBN, at a concentration of 0.02–0.04 mol/L, has been shown to be an important factor in the production of free methylene radicals in poly(BA) and free hydroxyl radicals in cellulosic macromolecule (Ayman et al. 2011; Alper and Nuran 2016). Nonetheless, increasing the concentration of the initiator AIBN beyond 0.04 mol/L reduces the graft process, because homo-polymeric interactions of BA promoted the viscosity of the reaction system (Ayman et al. 2011; Alper and Nuran 2016).

3.5 Effect of Cross-Link Agent Content on the Gel Fraction and Oil Sorption Capacity

Two well-known cross-linkers DVB and MBA in copolymers are very useful, in which they not only establish three-dimensional structure of materials, but also are mechanically robust, resistant to heat, wear, and solvent assault. The great value of these cross-linkers may due to the flexibility of terminal methylene groups in radical reactions (Prasetya et al. 2020; Atmanto et al. 2017). Under the above optimal conditions for the graft synthesis, in this scenario, we compare the effect of crosslinking agent rate and best type for the best GF and OSC values of DD-*g*-poly(BA). To do this, we created a variety of graft copolymer oil absorbents containing varying amounts of DVB and MBA (0.5–2.5%/monomer weight).

From Table 2, both the GF and OSC values increase and reach the maximal amounts of 97.4% and 23.56 g/g for DVB and 95.81% and 20.15 g/g for MBA, respectively, when the concentration of cross-linkers increases to 2.0%. This may be due to the viscosity effect oil and pore size of cross-linked oil sorbents. The lower concentration of DVB or MBA (less than 2%), on the other hand, would result in an oil absorbent with a too loose cross-linked network. As a result, there was a decrease in oil absorption. However, the amount of cross-linker DVB or MBA is over 2%, both the GF and OSC values decrease. Rationally, an overabundance of cross-linkers will result in the production of a copolymer network that is overly dense, and substantially reduce the chain length between cross-linked locations, and reduce the mobility of the polymeric chains (Mohamed et al. 2013a, 2013b). This is not advantageous for the oil to flow inside the network, thereby the absorbency is low. Overall, the GF and OSC in case of using cross-linker DVB is always higher than those of MBA. It suggests that the higher reactivity of DVB compared to MBA.

Table 2 The GF and OSC values of cross-linked graft copolymers using two different cross-linkers at various concentrations

Cross-link content (wt.%)	GF (%)		OSC (g/g)	
	DVB	MBA	DVB	MBA
0.5	69.40	62.91	14.50	13.42
1.0	75.60	70.12	18.70	15.67
1.5	80.20	78.29	20.80	17.78
2.0	97.50	95.81	23.56	20.15
2.5	96.80	94.72	16.7	14.56

3.6 FT-IR Spectroscopic Analysis

The FT-IR illustrations of DD and DD-*g*-poly(BA) have shown in Fig. 6. From Fig. 6, O–H stretching vibration of DD-*g*-poly(BA) sets as a small peak at 3441.10 cm^{-1}, as compared with a broad peak of 3434.11 cm^{-1} of original materia (Ensieh et al. 2022). In both two samples, the peaks at around 2900 cm^{-1} are assignable to C-H stretching. The broad peak at 1028.87 cm^{-1} in the FT-IR spectrum of DD material belongs to stretching vibration of O-C-O bond, whereas this vibration in the FT-IR image of DD-*g*-poly(BA) is found to reach a sharp peak at 1161.12 cm^{-1} (Nguyen et al. 2021b). In particular, a new strong-sharp peak at 1734.11 cm^{-1} in the FT-IR spectroscopy of DD-*g*-poly(BA) represents for carbonyl stretching of an ester, confirming the effective grafting (Ensieh et al. 2022).

3.7 Scanning Electron Microscopy (SEM) Analysis

SEM analysis of the cellulose from raw material DD revealed long and twisted fibers (Fig. 7). It is further observed that the DD surface is irregular, ruptured and cracked (Ibrahim et al. 2016). After grafting, the surface is almost covered with a heterogeneous grafting layer of monomer BA (Feng et al. 2009; Zuoxin et al.2009), the rough surface of DD becomes smooth in its co-polymer DD-*g*-poly(BA) (Fig. 7). The branches of BA grafted onto DD backbone randomly during the synthetic procedure, as well as most of them are vertical to the axis of backbone (Feng et al. 2009).

3.8 X-Ray Diffraction (XRD) Analysis

The X-ray diffraction illustrations of DD and DD-*g*-poly(BA) were demonstrated in Fig. 8. Regarding, the XRD image of DD, two peaks at 23.0 and 19.0° were accompanied by the relative intensities of 643.4 and 346.7

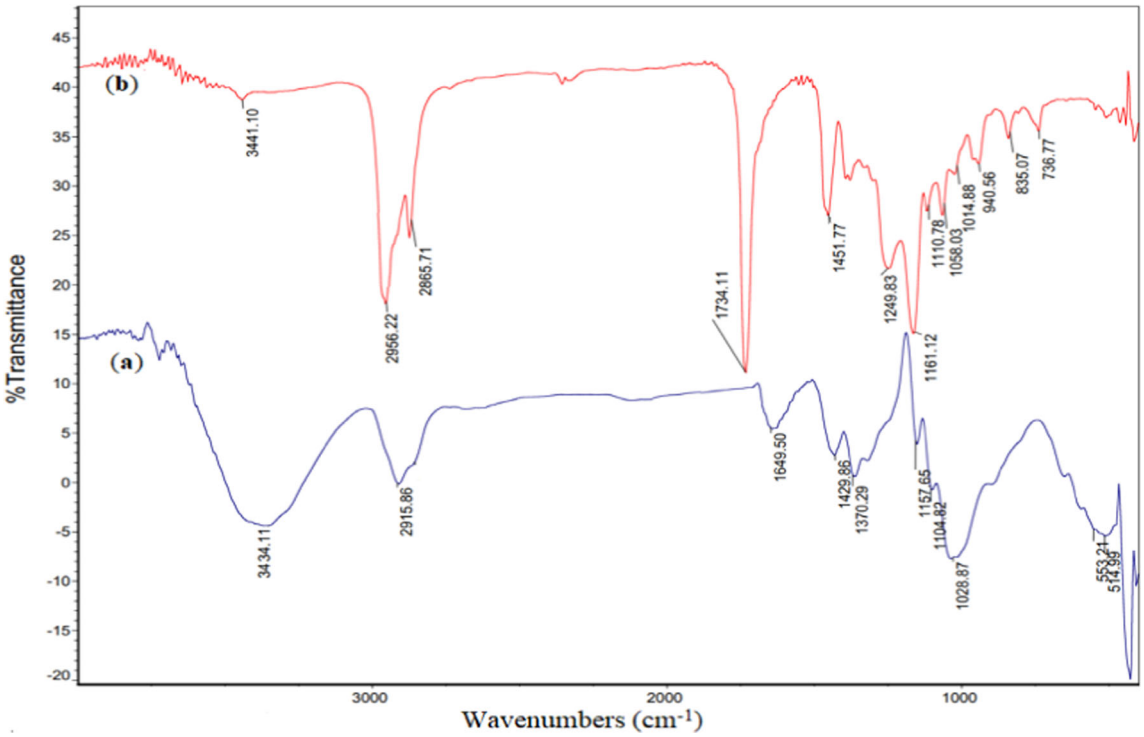

Fig. 6 The IR spectra of DD (**a**) and DD-*g*-poly(BA) (**b**)

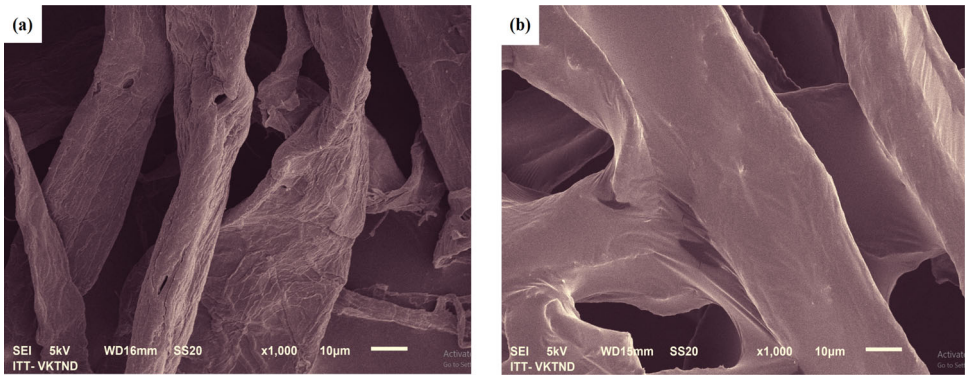

Fig. 7 SEM micrograph of DD (**a**) and DD-*g*-poly(BA) (**b**)

(a.u.), respectively. As compared with this, co-polymer DD-*g*-poly(BA) has also contained the same two peaks, but their relative intensities decrease up to 347.5 and 211.4 (a.u.). It suggests that the attachment of poly(BA) side chains to the cellulosic backbone can be a main reason for reducing crystallinity (Deepak et al. 2017).

3.9 Thermal Stability Analysis

As shown in Fig. 9, the thermogravimetric curves of DD and its copolymer are contingent upon the change in temperature. The thermal degradation of the cellulose of untreated material DD has been recorded in three phases (Fig. 9a). The first step associating with volatilization of moisture occurred at the temperature of less than 280 °C, and resulted in 6.726% weight loss (Mohamad et al. 2017; Shiguang et al. 2004). The degradation of cellulosic fibrils was then a second step, especially in terms of 353.65 °C (92.036% weight loss). Evidently, original material DD existed as a residual solid at 500 °C (Gao et al. 2012). Meanwhile, the disintegration of cellulose fibrils of DD-*g*-poly(BA) was observed to peak at 245.97 °C (Fig. 9b). Significantly, the weight loss process of DD-*g*-poly(BA) has so far consisted of a peak at 379.50 °C. The destruction of poly(BA) side chains is mainly reasonable for explanation (Gao et al. 2012).

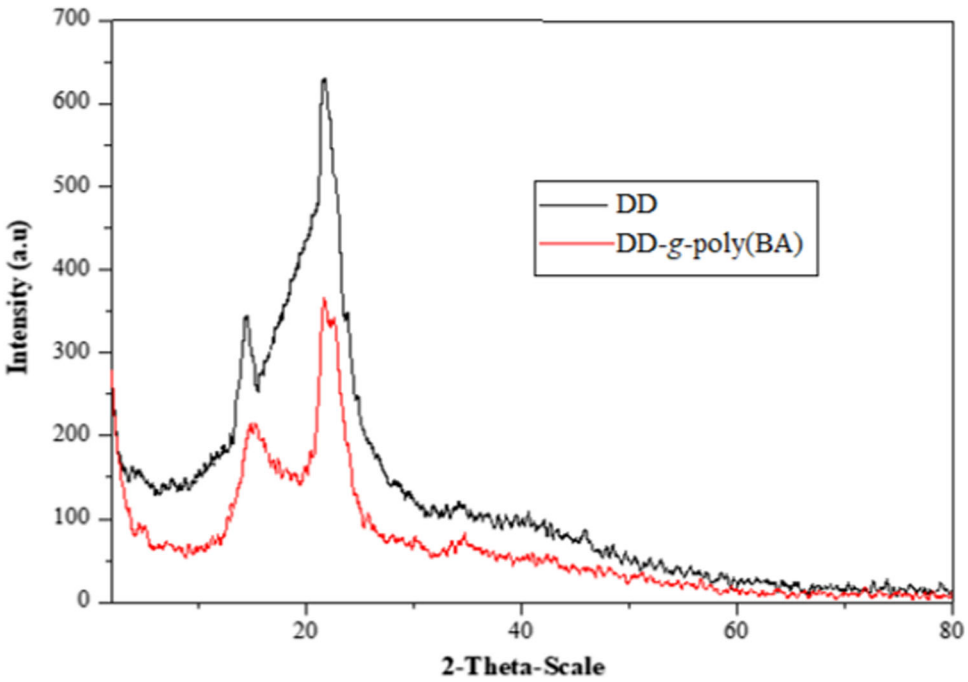

Fig. 8 The XRD patterns of DD and DD-*g*-poly(BA)

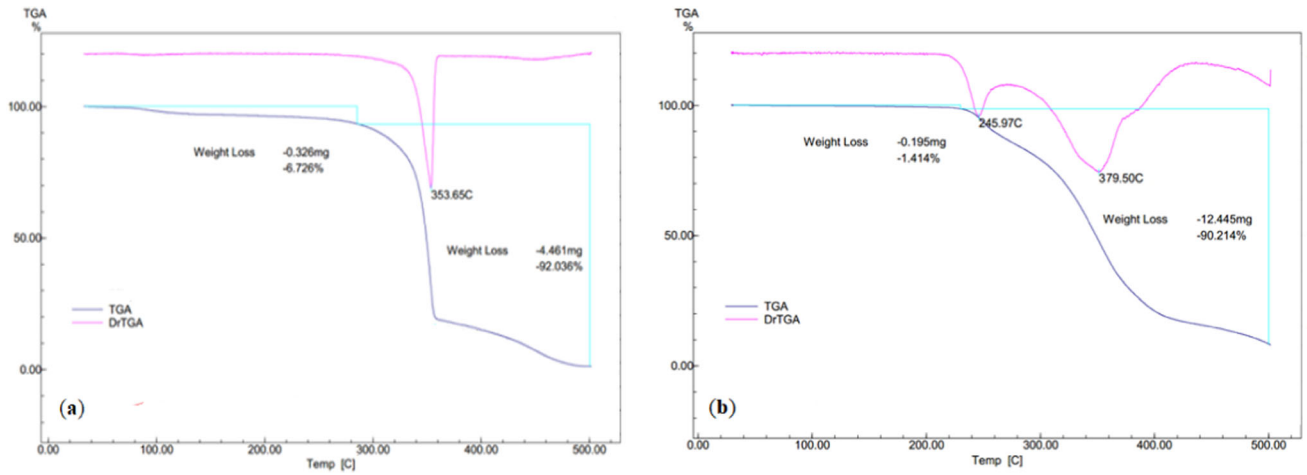

Fig. 9 TGA curve of DD (**a**) and DD-*g*-poly(BA) (**b**)

3.10 BET Surface Area Analysis

The results of BET surface area, and pore volume of DD fiber and its graft co-polymer DD-*g*-poly(BA) were outlined in Table 3. BET surface area and pore volume of the DD-*g*-poly(BA) are higher than those of DD raw material. This can be explained by the kinetic restrictions of nitrogen flow into their narrow micropores and DD-g-BA contained numerous micropores and mesopores, in contrast to that of DD raw material. The temperature also affects the porous structure. The temperature of the BA grafting reaction was around 75 °C. The long temperature treatment can lead to formation of new pores and enlargement of the existing ones. Inaccurate surface area measurements can result from nitrogen's interactions with non-polar surface functions because these interactions can cause nitrogen's pore filling pressure to drop dramatically. Since nitrogen was used to estimate the surface area, BET surface area value for DD-*g*-poly(BA) may be larger. Therefore, opening these pores

Table 3 BET surface area, and pore volume of DD and DD-*g*-poly(BA)

Samples	BET surface area (m^2/g)	Pore volume (cm^3/g)
DD	6.02	0.014
DD-*g*-poly(BA)	16.72	0.021

during the BA grafting procedures might help with oil uptake (Adilah et al. 2014; Wenbo et al. 2015).

3.11 Batch Oil Sorption

3.11.1 Effect of Contact Time

Figure 10 exhibits independence of the OSC on contact time. Both two samples possessed similar oil uptake behavior (similar shape but differ in size and position). In addition, the OCS of vegetable oil is always higher than that of crude oil. The vegetable oil with low viscosity is easier to diffuse into the network and retains in the porous structure (Thakur et al. 2013). The OSC curves of vegetable and crude oil uptake increase with time up, and achieve the high values of 25.63 g/g (vegetable oil) and 23.56 g/g (crude oil) at 25 min. After that, they become equilibrium (or near equilibrium state). This phenomenon can be caused by the sorption happening on the outside surface, which then penetrates the microscopic inside spaces (Vijay et al. 2013b).

3.11.2 Effect of Sorbent Dosage

Sorbent dosage may have an impact on the interaction between oil and sorbent. As shown in Fig. 11, there is an inverse relationship between the OSC and sorbent dosage. Sorbent dosage varies from 0.1 to 0.5 g, while the OSC values for both vegetable and crude oils are observed to be decreased. The influence of the initial dosage of sorbent is a key factor in the large scale of oil spill cleaning employment. Co-polymer DD-*g*-poly(BA) at the lowest dose of 0.1 g is associated with the maximal OSC values of 25.63 g/g (vegetable oil) and 23.56 g/g (crude oil), whereas the lowest OSC values are 10.0 g/g (vegetable oil) and 6.0 g/g (crude oil) at the dose of 0.5 g. This decrease is

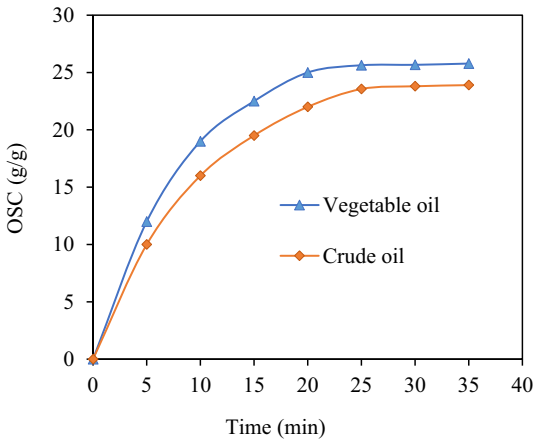

Fig. 10 Effect of contact time on the OSC. Sorbent dosage = 0.1 g and temperature = 40 °C

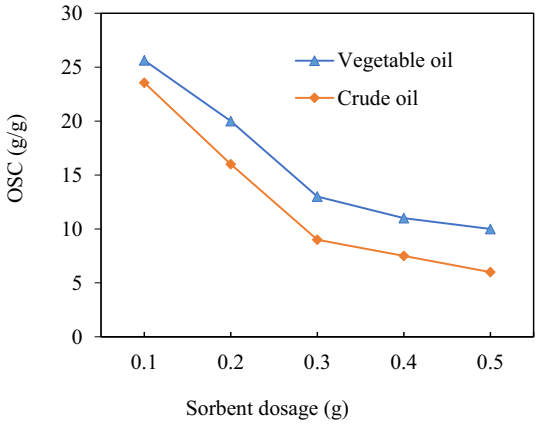

Fig. 11 Effect of sorbent dosage on the OSC. Contact time = 25 min and temperature = 40 °C

basically attributed to the remaining unsaturated active sites throughout the sorption process. When sorbent dose is increased while oil dosage remains constant can lead to a reduction in the oil adsorbed amount per unit weight of sorbent because of the residence of a restricted amount of oil per unit weight of the sorbents (Feng et al. 2014).

3.11.3 Effect of Sorption Temperature

The OSC values are marginally influenced by increasing the temperature from 25 to 55 °C, as shown in Fig. 11. A visible increase in the OSC values is found when temperature ranges from 25 to 40 °C. This result can be explained by the reduction of oil viscosity, since more energy is necessary for bounding oil molecules to sorbent surface (Rafeah et al. 2013). However, the connection of the oil molecules decreases, and unpredictability of oil sorption process happens after 40 °C, thereby the OCS values decreased (Rafeah et al. 2013). It possibly concludes that the sorption process occurs best at lower temperatures due to exothermic property. It also reflects the fact that the oil molecules diffuse at a faster rate with less time sorption (Qin et al. 2011). At higher temperatures, on the other hand, the boundary layer thickness reduces due to the strong tendency of oil molecules to migrate from the adsorbent surface to the bulk phase, resulting in a significant reduction in sorption trend. Aside from that, the oil molecules' total energy is increased, which improves their escape affinity (Fig. 12).

3.12 Hydrophobicity–Oleophilicity and Reusability

The sorption of both vegetable and crude oils of DD-*g*-poly(BA) in oil-over-water baths, including varied volume of oils, has been depicted in Fig. 13. The amount of water

picked up is also displayed, which indicates sorbent selectivity between water and oils. To date, no report discussed about this aspect regarding co-polymers/polymers containing DD material before. In both two cases, oil sorption increases with volume of oils added into the baths, until the equilibrium between sorbent and oils is almost reached. In agreement with above findings, at oil volume of 25 mL (oil–water, 1:10, v/v), our synthetic co-polymer possesses the highest vegetable oil sorption of 25.63 g/g and the lowest water sorption of 2.17 g/g (Fig. 13a). Meanwhile, it is associated with the highest crude oil sorption of 23.56 g/g and the lowest water sorption of 1.48 g/g (Fig. 13b). It can be safely concluded that hydrophobicity-oleophilicity of co-polymer DD-*g*-poly(BA) is always better than those of crude oil due to the higher viscosity.

The capacity of an oil sorbent material to recover absorbed oil is determined by its reusability. Superior oil sorbent material recycling performance helps lower the cost of oil pollution remediation. Figure 13 shows the OSC values of the co-polymer DD-*g*-poly(BA) for both vegetable and crude oils after seven sorption/desorption cycles. During each of seven cycles, the OSC is found to be decreased gradually. For the first cycle, the OCS values assigning to vegetable and crude oils are 25.63 g/g and 23.56 g/g, respectively. However, the reduction in the OCS for both vegetable and crude oils after seven cycles are 8.50 g/g (33.16%) and 6.20 g/g (26.31%). The mechanical irreversible deformation of partial fiber structure, the reduction in fiber interspace, and the presence of residual oil in fibers could all contribute to the reduction after each sorption/desorption cycle (Teik-Thye and Xiaofeng 2007). It is expected that the lowest environmental impact by decreasing sorbent waste via reuse of sorbents is also environmental protection (Fig. 14).

3.13 Oil Adsorption Isotherm and Kinetic Studies

Adsorption isotherm study allows to view the interactions between solute and adsorbent, in which Langmuir and Freundlich isotherm models should be suitable to investigate equilibrium (Ola et al. 2017; Emeka et al. 2010). The linear Langmuir model is proposed by Eq. 4:

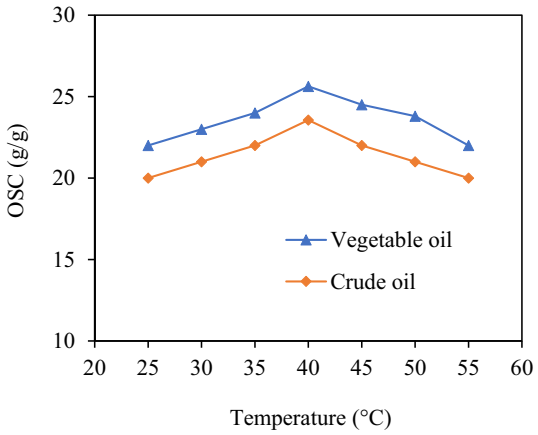

Fig. 12 Effect of oil temperature on the OSC. Sorbent dosage = 0.1 g and contact time = 25 min

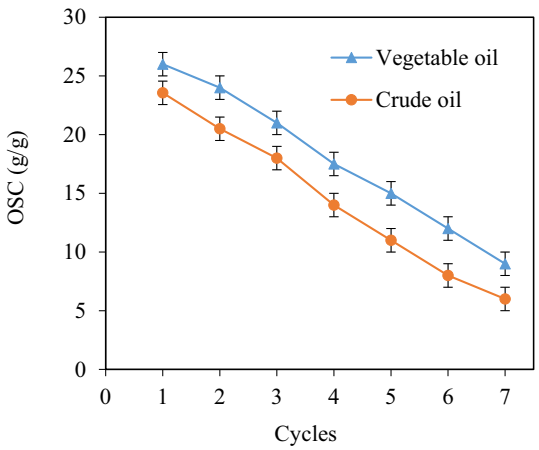

Fig. 14 Reusability of DD-*g*-poly(BA)

Fig. 13 Liquid sorption by DD-*g*-poly(BA) from oil-over-water as a function of oil volume for vegetable oil (**a**), crude oil (**b**)

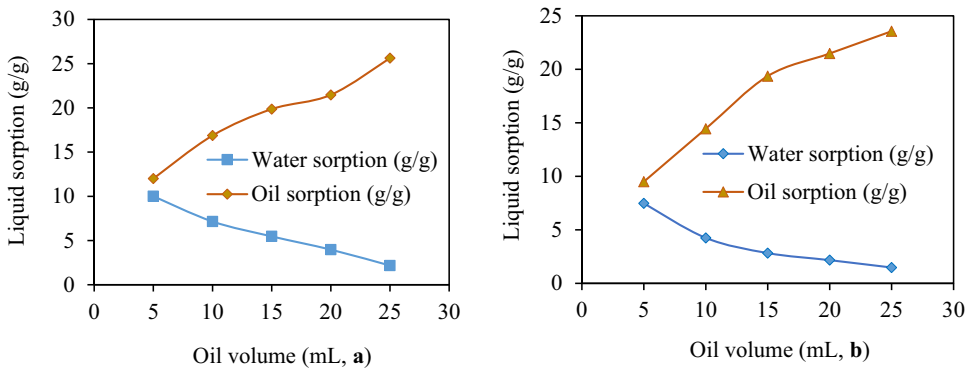

$$\frac{C_e}{q_e} = \frac{1}{q_{max} K_L} + \frac{C_e}{q_{max}} \quad (4)$$

where q_e represents the equilibrium concentration of oil in the adsorbed phase (g/g), while K_L is a constant involved in the adsorption energy. C_e denotes the equilibrium concentration of oil in the liquid phase (g/L), while q_{max} exhibits the monolayer capacity of absorbent (g/g).

The empirical Freundlich model describes heterogeneous systems which might be shown in its logarithmic Eq. 5:

$$\mathrm{Log} q_e = \mathrm{Log} K_F + \frac{1}{n} \log C_e \quad (5)$$

where the Freundlich constants K_F and n demonstrate the respective adsorption capacity and intensity. It should be noted that the absorption is remarkable with the slope n ranging from 2.0 to 10.0 (Emeka et al. 2010). Figure 15 shows the plots of C_e/q_e versus C_e, and log q_e versus log C_e, as well as the other values recorded in Table 4.

To investigate adsorption kinetics of vegetable and crude oils on DD-*g*-poly(BA), the obtained data have been so far examined with the pseudo-first and the pseudo-second-order models.

The linear pseudo-first-order has been generally shown by Eq. 6:

$$\mathrm{Log}(q_e - q_t) = \log q_e - \frac{k_1}{2.303} t \quad (6)$$

where q_e and q_t are the amounts of adsorbed vegetable oil or crude oil at equilibrium and time t (g/g), respectively. k_1 and t stand for the first-order constant (min^{-1}) and time (min), respectively. The linear pseudo-second is written by Eq. 7:

$$\frac{t}{q_t} = \frac{1}{k_2 q_e^2} + \frac{1}{q_e} t \quad (7)$$

where k_2 is the second-order constant (g/g min).

Table 4 Kinetic data for crude and vegetable oil sorption

Models	Parameters	Crude oil	Vegetable oil
Langmuir	q_{max}	23.56	25.63
	K_L	2.8935	3.0040
	R^2	0.9994	0.9990
Freundlich	K_F	4.5467	6.2511
	n	3.1377	3.1979
	R^2	0.9830	0.9839
Pseudo-first order	k_1	–0.1915	–0.3216
	q_e	7.1078	9.5773
	R^2	0.9351	0.9468
Pseudo-second-order	k_2	0.0881	0.0698
	q_e	7.9745	10.6952
	R^2	0.9898	0.9474

The plots of $\log(q_e - q_t)$ versus time t and t/q_t versus time t have been shown in Fig. 16. The q_e, k_1, and k_2 values are evaluated from the plots and provided in Table 4.

In agreement with above results, q_{max} of 23.56 and 25.63 g/g are assigned to crude and vegetable oil adsorption, respectively. The most striking feature is that the correlation coefficient R^2 is golden criterion to compare between the isotherm models (Ola et al. 2017; Emeka et al. 2010).

From Figs. 15 and 16 and Table 4, the R^2 values of 0.9994 (crude oil) and 0.9990 (vegetable oil) in the Langmuir model tend to be much closer to 1.0 than those values in the Freundlich model, as well as the R^2 values in the pseudo-second-order model are always higher than those in the pseudo-first-order. Therefore, the adsorption of DD-*g*-poly(BA) can be described as Langmuir monolayer, and chemisorption (Ola et al. 2017; Emeka et al. 2010).

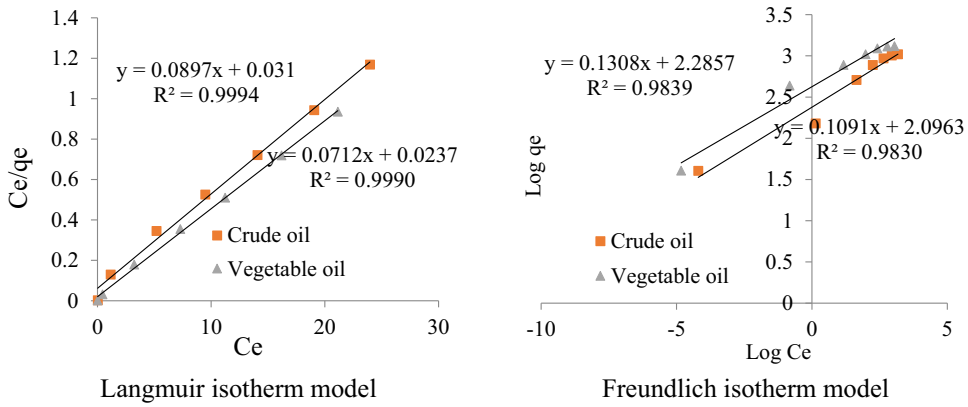

Fig. 15 The adsorption isotherm of DD-*g*-poly(BA) on vegetable and crude oils

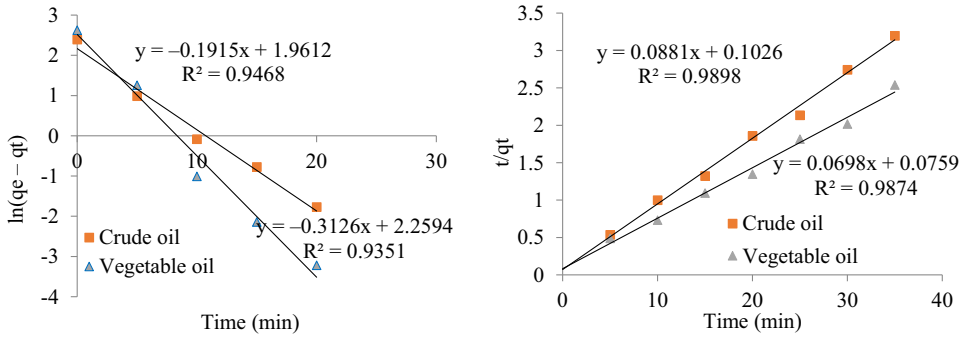

Fig. 16 The pseudo-first and second-order models of DD-*g*-poly(BA) on vegetable and crude oils

The pseudo-first order rate equation model The pseudo-second order rate equation model

4 Conclusion

The oil-sorbent DD-*g*-poly(BA) has been synthesized by graft co-polymerization of BA onto DD using initiator AIBN and cross-linking agent DVB or MBA. The highest GY value of 41.50% is associated with the optimal condition: C_{BA} = 1.50 mol/L, C_{AIBN} = 0.04 mol/L, 180 min, at 75 °C. The formation of co-polymer DD-*g*-poly(BA) is analytically characterized by FT-IR, SEM, XRD, thermal TGA, and BET surface area spectral data. In the presence of the DBV content of 1.50%, the maximal OSC values of this co-polymer toward crude and vegetable oils are 23.56 and 25.63 g/g. The batch study revealed that the sorption was a function of contact time (maximal at 25 min), sorbent dosage (maximal at 0.1 g), and temperature (maximal at 40 °C). Synthetic co-polymer shows remarkably hydrophobic and oleophilic properties, especially its reusability is accompanied by seven sorption/desorption cycles. Lastly, the oil absorption kinetics of DD-*g*-poly(BA) is possibly followed by Langmuir monolayer coverage and chemisorption.

Author Contributions NTT and NTS designated and wrote manuscript, NTD and PTTH, LDG, DXD performed experiments.

Funding The authors are grateful to Ministry of Industry and Trade (MOIT) via a project: ĐT.11.14/CNMT.

Data Availability The data used to support the findings of this study are available from the corresponding author upon request.

Declarations

Conflict of interest The authors declare that they have no conflict of interest.

Ethical Approval Our manuscript has not been submitted to more than one journal for simultaneous consideration. Our manuscript has not been published previously (partly or in full). A single study is not split up into several parts to increase the quantity of submissions and submitted to various journals or to one journal over time (e.g., "salami-publishing"). No data have been fabricated or manipulated (including images) to support your conclusions. No data, text, or theories by others are presented as if they were the author's own ("plagiarism"). Proper acknowledgments to other works must be given (this includes material that is closely copied (near verbatim), summarized, and/or paraphrased), quotation marks are used for verbatim copying of material, and permissions are secured for material that is copyrighted.

Informed Consent Our current study did not involve human subject, and has not used living animals, etc.

References

Adilah S, Nurhayati A, Syairah A (2014) Slow pyrolysis of oil palm empty fruit bunches for biochar production and characterisation. J Phys Sci 25:97–112

Alper A, Nuran I (2016) Microwave assisted synthesis and characterization of sodium alginate-graft-poly(N, N-dimethylacrylamide). Int J Biol Macromol 82:530–540. https://doi.org/10.1016/j.ijbiomac.2015.10.050

ASTM, D1533-00 (2005) Annual Book of ASTM Standards, vol. l0.3, American Society of Testing and Materials, Philadelphia

Atmanto HW, Ci R, Aprillia V, Ninis M, Agung T, Wijayanta HS (2017) Characterization of polypropylene itaconate in divinyl benzene and methylene bisacrylamide. Mater Chem Phys 186:552–560. https://doi.org/10.1016/j.matchemphys.2016.11.036

Ayman BM, Manuel RV, Albert M, Mohamed NB, Sami B (2011) Synthesis and characterization of cellulose whiskers/polymer nanocomposite dispersion by mini-emulsion polymerization. J Colloid Interface Sci 363:129. https://doi.org/10.1016/j.jcis.2011.07.050

Ching Khoo S, Phang XY, Ng CM, Lim KL, Lam SS, Ma NL (2019) Recent technologies for treatment and recycling of used disposable baby diapers. Process Saf Environ Prot 123:116–129. https://doi.org/10.1016/j.psep.2018.12.016

David WJ, Samuel MH (2001) Review of vinyl graft copolymerization featuring recent advances toward controlled radical-based reactions and illustrated with chitin/chitosan trunk. Chem Rev 101:3245–3273. https://doi.org/10.1021/cr000257f

Deepak P, Arush S, Vandana S (2017) Microwave induced graft copolymerization of binary monomers onto luffa cylindrica fiber: removal of congo red. Procedia Eng 200:408–415. https://doi.org/10.3389/fchem.2014.00059

Emeka TN, Gimba C, Kagbu JA, Nale BY (2010) Sorption studies of crude oil on acetylated rice husks. Arch Appl Sci Res 2:142–151

Ensieh GL, Sahar Y, Elaheh KA, Soheila S, Hossein J, Roshanak R-M, Thomas JW (2022) Polyvinyl alcohol/chitosan/silver nanofibers as antibacterial agents and as efficient adsorbents to remove methyl orange from aqueous solutions. J Iran Chem Soc 19:1287–1299. https://doi.org/10.1007/s13738-021-02382-x

Feng Y, Jun-fu W, En-qi T, Kongyin Z (2009) Synthesis of butyl acrylate grafted polypropylene fibre and its applications on oil-adsorption in floating water. E-Polymers. https://doi.org/10.1515/epoly.2009.9.1.1079

Feng L, Miaolian M, Deli Z, Zhengxin G, Chengyu W (2014) Fabrication of superhydrophobic/superoleophilic cotton for application in the field of water/oil separation. Carbohydr Polym 103:480–487. https://doi.org/10.1016/j.carbpol.2013.12.022

Frency SFN, Subramanian SM, Yi L, Hui PCL (2013) A critical review on life cycle assessment studies of diapers. Crit Rev Environ Sci Technol 43:1795–1822. https://doi.org/10.1080/10643389.2012.671746

Gao Y, Zhou Y, Zhang X, Qu P (2012) Synthesis and characteristics of graft copolymers of poly(butyl acrylate) and cellulose fiber with ultrasonic processing as a material for oil absorption. BioResources 7:135. https://doi.org/10.15376/BIORES.7.1.0135-0147

Hua L, Lifen L, Fenglin Y (2013) Oleophilic polyurethane foams for oil spill cleanup. Procedia Environ Sci 18:528–533. https://doi.org/10.1016/j.proenv.2013.04.071

Ibrahim HM, Mashiur RK, Mofakkharul I, Saiful I, Rabb MA (2016) Characterization of grafted jute fiber using acrylate monomers pretreated with alkali. Fash Text 3:9. https://doi.org/10.1186/s40691-016-0060-2

Jee KL, Julian M, Fatin NM, Soo KC, Kar BT, Oon JL (2021) New open-loop recycling approaches for disposable diaper waste. Environ Rev. https://doi.org/10.1139/er-2021-0033

Joan C, Maria M-M, Ignasi P-V, Antoni S (2013) Performance of compostable baby used diapers in the composting process with the organic fraction of municipal solid waste. Waste Manag 33:1097–1103. https://doi.org/10.1016/j.wasman.2013.01.018

Khandelwal H, Thalla AK, Kumar S, Kumar R (2019) Life cycle assessment of municipal solid waste management options for India. Biores Technol 288:121515. https://doi.org/10.1016/j.biortech.2019.121515

Khullar R, Varshney VK, Naithani S (2008) Grafting of acrylonitrile onto cellulosic material derived from bamboo (*Dendrocalamus strictus*). Express Polym Lett 2:12. https://doi.org/10.3144/expresspolymlett.2008.3

Mendoza JMF, D'Aponte F, Gualtieri D, Azapagic A (2019a) Disposable baby diapers: life cycle costs, eco-efficiency and circular economy. J Clean Prod 211:455–467. https://doi.org/10.1016/j.jclepro.2018.11.146

Mendoza JMF, Popa SA, D'Aponte F, Gualtieri D, Azapagic A (2019b) Improving resource efficiency and environmental impacts through novel design and manufacturing of disposable baby diapers. J Clean Prod 210:916–928. https://doi.org/10.1016/j.jclepro.2018.11.046

Mohamad JMF, Beddu S, Sadon SN, Kamal NLM, Itam Z, Mohamad K, Sapua W (2017) Disposable baby diapers: life cycle costs, eco-efficiency and circular economy. Indian J Sci Technol 10:1. https://doi.org/10.17485/ijst/2017/v10i4

Mohamed K, Thanaa A-M, Abdul-Raheim MA-R, Khalid IK, Hel-H S (2013a) Synthesis and characterization of oil sorbent based on Hydroxypropyl Cellulose Acrylate. Egypt J Pet 22:539–548. https://doi.org/10.1016/j.ejpe.2013.11.008

Mohamed K, Sabrnal H-H, Abdulraheim MAH, Khalid K, Thanaa A-M (2013b) Synthesis and evaluation of oil sorbent based on natural modified cellulose derivatives for treatment of oil spill. Elixir Org Chem 60:16081–16089

Nguyen TT, Nguyen TD, Pham TTH, Hoang TVA, Ninh TS, Le DG, An HTV, Son NT (2021a) A novel rice straw-butyl acrylate graft copolymer synthesis and adsorption study for oil spill cleanup from seawater. Cellulose Chem Technol 56(3–4):461–470. https://doi.org/10.35812/CelluloseChemTechnol.2022.56.39

Nguyen TT, Nguyen TD, Pham TTH, Ninh TS (2021b) Oil sorbent based on luffa fiber-graft-poly(butyl acrylate) copolymer. Iran J Sci Technol Trans Sci 45:1963–1970. https://doi.org/10.1007/s40995-022-01282-w

Nguyen TT, Nguyen TD, Pham TTH, Nguyen VK, Ninh TS (2022a) Graft polymerization of lauryl methacrylate onto bamboo fiber—a potential material for oil spills. Polym Polym Compos 30:1–7. https://doi.org/10.1177/09673911221093160

Nguyen TT, Nguyen TD, Pham TTH, Ninh TS (2022b) The graft copolymerization of butyl acrylate and lauryl methacrylate onto sawdust: potential materials for oil spill cleanup. Iran J Sci Technol Trans Sci 46:385–394. https://doi.org/10.1007/s40995-022-01282-w

Ola A, Samir MN, Walaa MT (2017) Palm fibers and modified palm fibers adsorbent for different oils. Alex Eng J 56:749–755. https://doi.org/10.1016/j.aej.2016.11.020

Prasetya NBA, Ngadiwiyana N, Ismiyarto I, Sarjono PR (2020) Effects of percent weight of divinylbenzene as crosslinking agent on the properties of eugenol–divinylbenzene copolymers. J Phys Conf Ser 1524:012089. https://doi.org/10.1088/1742-6596/1524/1/012089

Qin L, Li S, Ya Z, Yan Q, Jianping Z (2011) Characteristics of equilibrium, kinetics studies for adsorption of Hg (II) and Cr (VI) by polyaniline/humic acid composite. Desalination 266:188–194. https://doi.org/10.1016/j.desal.2010.08.025

Qinhui C, Xinggong M, Hanyu X, Yi D, Jinhuo L (2013) Preparation and characterization of bamboo fiber-graft-lauryl methacrylate and its composites with polypropylene. J Appl Polym Sci 130:2377. https://doi.org/10.1002/app.39347

Rafeah W, Luqman CA, Thomas CSY, Zainab N, Mohsen NM (2013) Oil removal from aqueous state by natural fibrous sorbent: an overview. Sep Purif Technol 113:51–63. https://doi.org/10.1016/j.seppur.2013.04.015

Saisai H, Qiufang J, Bin Y, Yujing N, Zhongqing M, Lingfei M (2019) Combined chemical modification of bamboo material prepared using vinyl acetate and methyl methacrylate: dimensional stability, chemical structure, and dynamic mechanical properties. Polymers 11:1651. https://doi.org/10.3390/polym11101651

Shiguang L, Shaoping X, Shuqin L, Chen Y, Qinghua L (2004) Fast pyrolysis of biomass in free-fall reactor for hydrogen-rich gas. Fuel Process Technol 85:1201–1211. https://doi.org/10.1016/j.fuproc.2003.11.043

Sotelo-Navarro PX, Poggi-Varaldo HM, Turpin-Marion SJ, Vázquez-Morillas A, Beltrán-Villavicencio M, Espinosa-Valdemar R (2017) Biohydrogen production from used diapers: evaluation of effect of temperature and substrate conditioning. Waste Manag Res 35:267–275. https://doi.org/10.1177/0734242X16677334

Teik-Thye L, Xiaofeng H (2007) Evaluation of kapok (*Ceiba pentandra* (L.) Gaertn.) as a natural hollow hydrophobic–oleophilic fibrous sorbent for oil spill cleanup. Chemosphere 66:955–963. https://doi.org/10.1016/j.chemosphere.2006.05.062

Thakur VK, Thakur MK, Gupta RK (2013) Graft copolymers from natural polymers using free radical polymerization. Int J Polym Anal 18:495–503. https://doi.org/10.1080/1023666X.2013.814241

Trilokesh C, Bavadharani P, Mahapriyadarshini M, Janani R, Uppuluri KB (2021) Recycling baby diaper waste into cellulose and nanocellulose. Waste Biomas Valori 12:4299. https://doi.org/10.1007/s12649-020-01312-x

Umberto A, Filomena A, Fabrizio DG (2016) Technological, environmental and social aspects of a recycling process of post-consumer absorbent hygiene products. J Clean Prod 127:289–301. https://doi.org/10.1016/j.jclepro.2016.03.164

Vijay KT, Manju KT, Raju KG (2013a) Development of functionalized cellulosic biopolymers by graft copolymerization. Int J Biol Macromol 62:44–51. https://doi.org/10.1016/j.ijbiomac.2013.08.026

Vijay KT, Manju KT, Raju KG (2013b) Graft copolymers from cellulose: synthesis, characterization and evaluation. Carbohydr Polym 97:18–25. https://doi.org/10.1016/j.carbpol.2013.04.069

Viju S, Brindha R, Thilagavathi G (2019) Surface modification of nettle fibers by grafting to improve oil sorption capacity. J Ind Text 50:1–16. https://doi.org/10.1177/1528083719862879

Wang J, Zheng Y, Wang A (2013) Coated kapok fiber for removal of spilled oil. Mar Pollut Bull 69:91–96. https://doi.org/10.1016/j.marpolbul.2013.01.007

Wenbo C, Xiaoyan L, Xinying Z, Beibei L, Tiantian Y, Junchen Z (2015) Preparation and characterization of polypropylene fiber-grafted polybutylmethacrylate as oil sorbent. Desalination 57:1–12. https://doi.org/10.1080/19443994.2015.1089195

Yue Z, Sheng Y, Jian-Quan W, Tong-Qi Y, Run-Cang S (2014) Preparation and characterization of lignocellulosic oil sorbent by hydrothermal treatment of populus fiber. Materials 7:6733–6747. https://doi.org/10.3390/ma7096733

Zuoxin L, Yonggang M, Zhenying W, Guanghua Y (2009) Synthesis and characterization of a novel super-absorbent based on chemically modified pulverized wheat straw and acrylic acid. Carbohydr Polym 77:131–135. https://doi.org/10.1016/j.carbpol.2008.12.019